Journal of Nuclear Medicine, published on December 17, 2015 as doi:10.2967/jnumed.115.166975

Molecular-Guided Endoscopy Targeting Vascular Endothelial Growth Factor A for Improved Colorectal Polyp Detection

Jolien J Tjalma[1*], P Beatriz Garcia-Allende[2*], Elmire Hartmans[1], Anton G Terwisscha van Scheltinga[3], Wytske Boersma-van Ek[1], Jürgen Glatz[2], Maximilian Koch[2], Yasmijn J van Herwaarden[4], Tanya M Bisseling[4], Iris D Nagtegaal[5], Hetty Timmer-Bosscha[6], Jan Jacob Koornstra[1], Arend Karrenbeld[7], Jan H Kleibeuker[1], Gooitzen M van Dam[8], Vasilis Ntziachristos[2], Wouter B Nagengast[1]

[*]Both contributed equally

University of Groningen, University Medical Center Groningen, Groningen, the Netherlands, [1]Department of Gastroenterology and Hepatology, University of Groningen, University Medical Center Groningen, Groningen, the Netherlands; [2]Chair for Biological Imaging & Institute for Biological and Medical Imaging, Technical University of Munich and Helmholtz Center Munich, Munich, Germany; [3]Department of Clinical Pharmacy and Pharmacology, University of Groningen, University Medical Center Groningen, Groningen, the Netherlands; [4]Department of Gastroenterology and Hepatology, Radboud University Medical Center, Nijmegen, the Netherlands; [5]Department of Pathology, Radboud University Medical Center, Nijmegen, the Netherlands; [6]Department of Medical Oncology, University of Groningen, University Medical Center Groningen, Groningen, the Netherlands; [7]Department of Pathology, University of Groningen, University Medical Center Groningen, Groningen, the Netherlands; and [8]Department of Surgery, University of Groningen, University Medical Center Groningen, Groningen, the Netherlands.

Authors disclosures of potential conflicts of interest

The authors have no conflict of interest, no financial interest and no arrangement or affiliation with any commercial organization that may have a direct or indirect interest in the content of this manuscript.

Correspondence

W.B. Nagengast, MD PhD
Dept. of Gastroenterology and
and Hepatology, BB41
University Medical Center Groningen
PO box 30.001
9700 RB Groningen
The Netherlands
E-mail: w.b.nagengast@umcg.nl
Phone: 0031 50 366 8335
Fax: 0031 50 361 9306

First author

J.J.J. Tjalma, MD
Dept. of Gastroenterology
Hepatology, BB41
University Medical Center Groningen
PO box 30.001
9700 RB Groningen
The Netherlands
E-mail: jjj.tjalma@umcg.nl
Phone: 0031 50 361 2620
Fax: 0031 50 361 9306

Word count

4969 words

Financial support

The research leading to these results was partially supported by the European Union under the grant agreement ERC-OA-2012-PoC-324627 and partially supported by the Dutch Cancer Society, RUG 2012-5416.

ABSTRACT

Small and flat adenomas are known to carry a high miss-rate during standard white-light endoscopy. Increased detection rate may be achieved by molecular-guided endoscopy with targeted near-infrared (NIR) fluorescent tracers. The aim of this study was to validate vascular endothelial growth factor A (VEGF-A) and epidermal growth factor receptor (EGFR) targeted fluorescent tracers during *ex vivo* colonoscopy with a NIR endoscopy platform.

Methods: VEGF-A and EGFR expression was determined by immunohistochemistry on a large subset of human colorectal tissue samples: 48 sessile serrated adenomas/polyps (SSA/P), 70 sporadic high-grade dysplastic (HGD) adenomas, 19 hyperplastic polyps (HP) and tissue derived from patients with Lynch syndrome (LS): 78 low-grade dysplastic (LGD) adenomas, 57 HGD adenomas and 31 colon cancer samples. To perform an *ex vivo* colonoscopy procedure, 14 mice with small intraperitoneal EGFR-positive HCT116^{luc} tumors received intravenously bevacizumab-800CW (anti-VEGF-A), cetuximab-800CW (anti-EGFR), control tracer IgG-800CW or sodium chloride. Three days later, 8 resected HCT116^{luc} tumors (2-5 mm) were stitched into one freshly resected human colon specimen and followed by an *ex vivo* molecular-guided colonoscopy procedure. **Results:** Immunohistochemistry showed high VEGF-A expression in 79-96% and high EGFR expression in 51-69% of the colorectal lesions. Both targets were significantly overexpressed in the colorectal lesions compared to the adjacent normal colon crypts. During *ex vivo* molecular-guided endoscopy all tumors could clearly be delineated for both bevacizumab-800CW and cetuximab-800CW tracers. Specific tumor uptake was confirmed with fluorescent microscopy showing respectively stromal and cell membrane fluorescence. **Conclusion:** VEGF-A is a promising target for molecular-guided fluorescence endoscopy as it showed a high protein expression, especially in SSA/P and LS. We demonstrate the feasibility to visualize small tumors real-time during colonoscopy using a NIR fluorescence

endoscopy platform, providing the endoscopist a wide-field ‘red-flag’ technique for adenoma detection. Clinical studies are currently being performed in order to provide in-human evaluation of our approach.

Keywords Optical Imaging; Molecular Imaging; Vascular Endothelial Growth Factor A; Near Infrared Fluorescence; Endoscopy.

White-light endoscopy is the gold standard for detection of premalignant and malignant colorectal lesions (*1*). Despite the efficacy of current colonoscopy, small and especially right-sided flat or serrated adenomas are notoriously difficult to detect, resulting in substantial polyp detection miss-rates of 20-26% (*2,3*). Missed lesions are a main risk factor for the occurrence of interval cancers, particularly in high-risk patients such as patients with Lynch syndrome (LS) (*4-6*). Advanced endoscopic imaging modalities, like narrow-band imaging, autofluorescence imaging and chromoendoscopy have been extensively investigated, but did not show significant improvement in adenoma detection rates (*7-9*). Ideally, white-light endoscopy is combined with a sensitive, wide field of view, 'red-flag' technique to assist the endoscopist in the immediate identification of aberrant lesions. Molecular optical imaging, *i.e.* visualizing the molecular signature of cells *in vivo*, would be highly suitable for this aim. It enables real-time anatomical and functional imaging and it is safe, fast and relatively inexpensive (*10*). With the use of selective optical agents functioning in the near infrared (NIR) light spectrum, contrast between normal mucosa and dysplastic tissue could potentially be greatly enhanced, thereby reducing miss-rates (*11*). These agents should target biomarkers known to be overexpressed in colorectal cancer like epidermal growth factor receptor (EGFR) or shown to be overexpressed early in the adenoma-carcinoma sequence, as described for vascular endothelial growth factor A (VEGF-A), due to the angiogenic switch (*12,13*). The aim of the current study was to validate VEGF-A and EGFR-targeting fluorescent antibodies in visualizing small colorectal lesions real-time with our novel NIR endoscopy platform. Therefore, we first determined the expression of potential targets VEGF-A and EGFR in archival human colorectal samples, including sessile serrated adenomas/polyps (SSA/P) and adenomatous and carcinomatous tissue of patients with LS.

Secondly, we performed a simulated endoscopy procedure to validate our VEGF-A and EGFR targeting NIR fluorescent tracers.

MATERIALS AND METHODS

Immunohistochemistry of Human Colorectal Lesions

The archival formalin-fixed and paraffin-embedded human colorectal tissue set consisted of: sessile serrated adenomas/polyps (SSA/P) (n=48; 42 different individuals), Lynch low-grade dysplasia (LGD) adenomas (n=78; 62 individuals), Lynch high-grade dysplasia (HGD) adenomas (n=57; 40 individuals), Lynch colon cancer tissue (n=32; 31 individuals), sporadic adenomas with HGD (n=70; 70 individuals) and hyperplastic polyps (HP) (n=19; 18 individuals). The tissue was handled according to Dutch Code of Conduct for proper use of Human Tissue (www.federa.org) and the study was conducted according to the guidelines of the medical ethical committee of our hospital (www.ccmo.nl). To evaluate the clinical relevance of an anti-VEGF and anti-EGFR fluorescent tracer for colorectal surveillance, the protein expression of VEGF-A and EGFR was determined by immunohistochemistry (IHC). Slides were rehydrated via graded alcohols. Antigen retrieval was retrieved with 0.100M Tris/HCl (pH 9.0, 15 minutes) for VEGF and 0.1% Proteinase K (30 minutes) for EGFR. Endogenous peroxidase blocking was performed during 30 minutes with 0.42% hydrogen peroxide, followed by avidin-biotin blocking. For VEGF, sections were incubated for one hour with polyclonal rabbit anti-human VEGF-A (Santacruz) (1:50) and consecutive for 30 minutes with swine anti-rabbit biotin (1:300 in phosphate-buffered saline (PBS) with 1% bovine serum albumin (BSA)) and Streptavidin (1:300 in PBS/1% BSA). For EGFR, sections were incubated for one hour with monoclonal mouse anti-EGFR (clone 31G7, Invitrogen) (1:50 in PBS/1% BSA) and consecutive for 30 minutes with rabbit anti-mouse peroxidase (1:100) and goat anti-rabbit peroxidase (1:100). Color development

was achieved by applying a 3-3'-diaminobenzine-tetrahydorchloride (DAB) reagent (Sigma) for 10 minutes. PBS was used throughout for washing and all steps occurred at room temperature. Finally, sections were counterstained with Mayer's hematoxylin, dehydrated in alcohol and coverslipped. Staining intensities were independently evaluated by two individuals; consensus was achieved in discrepant cases by consulting an experienced pathologist. Dysplasia, cancer and adjacent normal epithelium, if present, were separately scored and compared. Staining intensities were graded using a 0-3 scale (0 = completely negative, 1 = weak, 2 = moderate, 3 = strong staining).

Cell Culture

The HCT116^{luc} human colon cancer cell line, stably transfected with the firefly gene *luciferase*, was obtained from Caliper Life Sciences. The cells were grown in a monolayer culture using McCoy's 5A Medium (Gibco®, Life Technologies) supplemented with 10% fetal bovine serum, in a humidified atmosphere containing 5% CO_2 at 37°C. EGFR cell surface expression was confirmed for HCT116^{luc} (data not shown) with the use of fluorescence activated cell sorting (FACS; BD FACS Calibur, BD Biosciences).

Fluorescent Labeling of Monoclonal Antibodies

As described previously, the monoclonal antibodies bevacizumab (Roche), cetuximab (Merck) and human IgG (Nanogram, Sanquin) were labeled with IRDye800CW-NHS (LI-COR Biosciences) (*14,15*). This NIR fluorescent dye underwent extensive toxicity testing and is a GMP compliant compound, registered at the U.S. Food and Drug Administration (*16,17*).

HCT116^{luc} Human Xenograft Tumors

All experiments were approved by the animal welfare committee of the University of Groningen and carried out in accordance with the Dutch Animal Welfare Act of 1997. To obtain multiple small tumor lesions, fourteen male athymic nude mice (Harlan, Horst, the Netherlands) received an intraperitoneal (IP) injection with 200µL of $2x10^6$ $HCT116^{luc}$ cells suspended in PBS. Tumor growth was monitored with the use of IP injections with D-luciferin reconstituted in PBS (1.5 mg in 100 µl; PerkinElmer), followed by bioluminesence imaging with an *in vivo* imaging system (IVIS Spectrum; Caliper Life Sciences). At day 14 all mice reached bioluminescent signals indicating sufficient tumor growth, where after 100 µg bevacizumab-800CW (n=5), 100 µg cetuximab-800CW (n=5), 100 µg human IgG-800CW (n=2) or sodium chloride (n=2) was injected in a total volume of 200 µl. Intravenous injection was performed via the penile vein under general anesthesia. The mice receiving IgG-800CW or sodium chloride served as negative controls. At day 3 post injection mice were euthanized by cervical dislocation and eight small IP tumors (2-5 mm) were harvested for *ex vivo* colonoscopy purposes (2 per tracer). The remaining IP tumors (varying in size between 2 and 5 mm) and mouse organs (liver, colon and muscle) were harvested for *ex vivo* analyses.

NIR Fluorescence Endoscopy Platform

The NIR fluorescence endoscopy platform consists of a custom-made Micrendo® fiber-bundle containing 30,000 coherently-arranged individual fibers (Schölly Fiberoptic GmbH). The imaging bundle conducts the images to the sensor module of a previously developed clinical prototype NIR camera system (*18,19*). This camera system comprises of a color camera and a monochrome one, which operate in parallel for white-light and NIR fluorescence acquisition respectively. A beam splitter (T760lpxr, Chroma Technology) separates the color and NIR image components. Appropriate filtering is provided by a white light shortpass filter with a cut-off

wavelength of 750 nm and a fluorescence emission bandpass filter with a central wavelength of 819 nm (bandwidth 44 nm) (THORLABS). Connection of the fiber-bundle to the camera system is made feasible via a mechanical and focusing adapter, while a multi-branched fiber optic bundle (SEDI-ATI Fibres Optiques) realizes simultaneous white-light illumination and fluorescence excitation (laser at 750 nm) coupling. The performance of the clinical endoscopy platform, namely the characterization of the optical resolution and the sensitivity, was determined as for the preclinical platform (*20*).

Simulation of a Molecular-Guided NIR Fluorescence Endoscopy Procedure

To simulate a clinical colonoscopy procedure, an 11 cm long human colon specimen was derived from a right hemicolectomy of a patient with colon cancer (requirement to obtain informed consent was waived by the Medical Ethical Committee Groningen, METC nr. 2013.446). Immediately after the surgical resection, the healthy part of the colon specimen was transported to the endoscopy suite. Two freshly resected $HCT116^{luc}$ IP tumors (2-5 mm in diameter) per tracer (bevacizumab-800CW, cetuximab-800CW, IgG-800CW or sodium chloride) were stitched onto the luminal side of the colon wall (Fig. 1). Molecular-guided fluorescence endoscopy was performed using a clinical video endoscope (Olympus Exera II GIF-180 series, Olympus), with the fiber-bundle of the NIR fluorescence endoscopy platform inserted through the working channel. The images were displayed on two separate screens, one for the video endoscope derived images and the other for the composite images of the fiber-bundle, combining color and fluorescence. A qualitative assessment of tumor visualization was made during endoscopy and video footage and photo material was collected.

***Ex Vivo* Analyses**

To further validate the findings of the simulated endoscopy procedure, the remaining harvested HCT116^{luc} human xenograft tumors, mouse organs and a part of the human colon tissue were formalin-fixed and paraffin-embedded for microscopic analysis. To detect if 800 nm fluorescence signals were present, 4 μm slides were obtained, deparaffinized (10 minutes xylene), scanned on an Odyssey Infrared Imaging System (intensity 5; LI-COR Biosciences) and subsequently hematoxylin&eosin (H&E) stained. Hoechst staining (33258; Invitrogen) was used to visualize nuclei for fluorescence microscopy. Analysis was performed using a Leica DM6000B inverted wide-field microscope (63x magnification, immersion oil); with a mercury short-arc reflector lamp (HXP-R120W/45C VIS), Leica DFC365FX camera and the filter set 49037ET of Chroma Technology. Images were processed with LAS-AF2 software (Leica Microsystems).

Statistical Analysis

Statistical analysis was performed using IBM SPSS Statistics 20. Per tissue type, the difference in staining intensity between aberrant tissue and adjacent normal tissue was determined via non-parametric Mann-Whitney U testing. The correlation between histological stage of Lynch tissue (LGD adenomas, HGD adenomas and cancer tissue) and staining intensity (0-3) was tested using a Kruskal Wallis test, corrected for multiple testing. Data are presented using Prism (version 5; GraphPad Software) and Adobe Illustrator CS6.

RESULTS

High VEGF-A Expression in Human Colorectal Lesions

IHC for VEGF-A showed a homogeneous staining pattern within dysplastic and carcinomatous areas (Fig. 2 and Suppl. Fig. 1A). From normal colon crypts towards dysplastic

and cancerous areas, a gradually increasing staining intensity was observed (Suppl. Fig. 1B). Moderate to strong VEGF-A expression was observed in 96% of Lynch LGD adenomas, 79% of Lynch HGD adenomas, 94% of Lynch colon cancer tissue and 94% of SSA/P. No significant differences in staining intensities could be observed between the different histological stages (LGD, HGD, carcinoma) of the LS samples. In addition, VEGF-A demonstrated to be a relevant target for other polyps as well, showing a 94% VEGF-A expression in HGD sporadic adenomas and 95% in HP lesions (Fig. 3). For all adenomas, the VEGF-A expression was significantly higher compared to the adjacent normal colonic crypts ($P < 0.001$), signifying the potential of this target for adenoma detection.

The percentage of EGFR positive samples was lower for all tissue types: 52% of Lynch LGD adenomas, 51% of Lynch HGD adenomas, 68% of Lynch cancer samples, 52% of SSA/P lesions, 51% of sporadic HGD adenomas and 58% of HP lesions showed a positive receptor staining (Fig. 3). In contrast to VEGF-A, EGFR IHC results showed a heterogeneous expression pattern throughout the neoplastic lesions, resulting in EGFR both negative and positive crypts within one adenoma (Fig. 2 and Suppl. Fig. 1A). The EGFR expression was significantly higher when compared to the adjacent normal colon crypts ($P < 0.001$). A gradient of increased EGFR expression from normal towards dysplastic crypts was not observed.

Performance of the NIR Fluorescence Endoscopy Platform

The resolution of the fluorescence endoscopy platform was characterized by imaging the USAF 1951 resolution test chart with the system's color channel (Fig. 4A). Here we can distinctly identify the vertical and horizontal lines in Element 3 of Group 1, which translates to a spatial resolution of 198.42 μm at a distance of 2 cm. The signal-to-noise ratios (SNR) were determined for a dilution series of IRDye800CW with concentrations ranging between 26.05 μM

and 1.55 pM (Fig. 4B). Each subsequent dilution was obtained of a halved concentration of IRDye800CW dissolved in PBS. The detection limit was defined as the concentration where the signal is three times higher than the noise, which corresponds to a SNR of 9.5 dB. The regression line is depicted in red. The detection limit, calculated from the regression line, lies at a concentration of 19.80 nM.

Ex Vivo Colonoscopy Procedure: Real-time Visualization of NIR Fluorescent Lesions

During the *ex vivo* colonoscopy procedure, the NIR fluorescence endoscopy platform exhibited sufficient sensitivity and resolution for the visualization of all small HCT116^{luc} tumors that were labeled with bevacizumab-800CW and cetuximab-800CW (Fig. 5 and Suppl. Fig. 2 and Suppl. Video 1). The endoscopist was able to instantly detect the specifically targeted tumors (2-5 mm) and differentiate these from the control tumors. White-light, fluorescence and composite images were displayed real-time and with a wide field of view. Fluorescence was also clearly visible when the fiber was retracted to a larger distance (~5 cm) of the fluorescent tumors. Control tumors from mice that were given IgG-800CW or sodium chloride showed negligible fluorescence signals and there was no interference of autofluorescence of the human colon tissue.

IRDye800CW-Labeled Tracers: *Ex Vivo* Established Target Specificity

Odyssey imaging system and fluorescence microscopy

Ex vivo macroscopic NIR fluorescence imaging of the deparaffinized tissue slides revealed highly fluorescent tumors with clear tumor delineation (Fig. 6B and Suppl. Fig. 3B) for both bevacizumab-800CW and cetuximab-800CW. IgG-800CW and negative tumors showed low autofluorescence signals (Suppl. Fig. 3E). NIR fluorescence was low in the HE-confirmed necrotic areas of the tumors and healthy adjacent mouse tissue (Figs. 6A and Suppl. Fig. 3A and

3D, orange arrows). Fluorescence microscopy confirmed the localization of bevacizumab-800CW and cetuximab-800CW in the vital parts of the HCT116^{luc} tumors (Fig. 6C and Suppl. Fig. 3C). For bevacizumab-800CW, the fluorescent signal was mainly located in the tumor stroma and surrounding the tumor blood vessels, corresponding with our previous observations for ^{89}Zr- and ^{111}In-labeled bevacizumab (*14,21*). A more homogeneous distribution was seen for cetuximab-800CW in the tumor lesions, with membranous and cytoplasmic localization of the NIR fluorescence signals (*22*).

DISCUSSION

This study demonstrates, in a simulation model, that it is feasible to visualize colorectal lesion in real-time, using a novel fluorescence endoscopy platform combined with VEGF-A and EGFR targeting NIR fluorescent tracers. Given the observed overall VEGF-A overexpression in colorectal lesions, this target appears to be the most relevant for molecular colorectal screening purposes. Especially in colorectal lesions that are easily missed during endoscopy, such as SSA/P lesions and Lynch adenomas, VEGF-A was highly overexpressed. The ability to visualize colon lesions in the simulation model used in this study, in combination with the GMP production of 800CW-labelled antibodies, allows rapid translation of this technique towards the clinic.

To the best of our knowledge, no prior data are available on VEGF-A expression in sessile serrated adenomas/polyps or neoplastic lesions from high-risk patients, like those with LS. We found a moderate to strong VEGF-A expression in the majority of SSA/P and Lynch adenomas. The high VEGF-A expression in sporadic adenomas was in concordance with literature (*12,13*). VEGF-A expression was significantly higher in adenoma crypts compared to adjacent normal colon crypts, which is a key requirement for successful visualization of target lesions by molecular imaging. Moreover, we observed a gradually increased staining intensity

from normal colon crypts towards dysplastic and cancerous areas in many of the samples, which can be explained by the fact that VEGF-A expression is regulated by several growth factors present in the microenvironment of premalignant and malignant lesions (*23*).

In contrast, EGFR is overexpressed in only ~50% of all adenoma lesions, including those of LS patients, and was expressed more heterogeneously throughout the lesions. The observed EGFR expression is in line with previous findings in sporadic adenomas (*24*). Therefore, VEGF-A seems the most suitable target for screening purposes. In contrast, cetuximab-800CW may still be valuable in evaluating the EGFR expression-status of an already identified lesion. In this setting, our approach could play an assisting role in molecular treatment decision-making processes, whereas EGFR-targeting therapeutics are currently being applied in colorectal carcinomas.

The use of a fiber-bundle based approach is relatively cheap and can easily be incorporated in standard clinical endoscopy procedures, as the fiber-bundle fits through the working channel of a routine clinical video endoscope. Although the fiber images have a significant lower resolution compared to high definition (HD) video endoscope images, the molecular-guided approach is very sensitive and provides strong contrast between the NIR fluorescent-targeted lesions and the surrounding normal tissue. Since the images are real-time and with a wide field of view, this approach can assist in the screening of large surfaces, with the white-light HD endoscope providing morphological orientation while the fiber can support as a red flag method.

The technique described in this study has several advantages when compared to other molecular-guided endoscopy approaches. First, confocal laser endomicroscopy, has shown both promising results preclinically and clinically, but has a limited field of view (*25-27*). Therefore, confocal laser endomicroscopy is not suitable for screening purposes, as our technique is, but rather a tool for lesion characterization. Secondly, other research groups have described topical

spraying of tracer products to improve detection of dysplastic regions, but this is most attractive for relatively small areas and therefore not practical in the colon (*28-30*). An approach using intravenously injected tracers can circumvent these issues. Finally, the use of a fluorescent tracer emitting in the NIR light spectrum likely improves specificity and tumor-to-background signals when compared to fluorescent dyes of the visible spectrum, since autofluorescence is negligible in the NIR range (Suppl. Figs. 4 and 5) (*31*).

Previously, in an HCT116^{luc} xenograft model, a TBR of 3.2±0.9 was seen for bevacizumab-800CW and 5.7±3.0 for cetuximab-800CW three days post injection (Suppl. Fig. 4). However, the commonly used tumor-to-background ratio cannot be reliable evaluated in mice, since the tracers are targeted towards human VEGF-A and EGFR. As a consequence, the used artificial model, targeted IP xenograft tumors stitched in a human colon specimen, demonstrates the practical feasibility of the proposed technique, but no statements can be made regarding specific tumor or adenoma accumulation in comparison to uptake in healthy human colon tissue. However, clinical studies evaluating the use of ^{89}Zr-labeled bevacizumab in breast- and kidney cancer patients did not show aspecific accumulation of the tracer in the colon (*32*). Also, the significant higher VEGF-A expression in colorectal adenomas compared to adjacent normal tissue implies that bevacizumab-800CW could be a promising tracer from a diagnostic point of view. The initiated clinical studies (NCT01972373 and NCT02113202) should give insight into the *in vivo* sensitivity and specificity of bevacizumab-800CW towards VEGF-A in different colorectal lesions, as well as the safety and optimal tracer dose to perform the molecular-guided endoscopy procedure.

CONCLUSION

Molecular-guided NIR fluorescence endoscopy is a promising technique that allows real-time, wide-field visualization of both tissue morphology and molecular characteristics. In this study we demonstrated that our GMP-produced NIR tracers, targeting VEGF and EGFR, could be clearly visualized during a simulated molecular-guided NIR fluorescence endoscopy procedure. Based on the expression profiles observed in a large set of different colorectal samples, including those in high-risk patients with SSA/P and Lynch syndrome, VEGF-A seems a suitable target for molecular-guided endoscopic screening purposes. Clinical studies have been initiated and are currently recruiting patients to validate the potential of this technology during colonoscopy (clinicaltrials.gov: NCT01972373 and NCT02113202).

DISCLOSURE

The research leading to these results was partially supported by the European Union under the grant agreement ERC-OA-2012-PoC-324627 and partially supported by the Dutch Cancer Society, RUG 2012-5416.

REFERENCES

1. Rockey DC, Paulson E, Niedzwiecki D, et al. Analysis of air contrast barium enema, computed tomographic colonography, and colonoscopy: prospective comparison. *The Lancet*. 2005;365:305-311.

2. Heresbach D, Barrioz T, Lapalus M, et al. Miss rate for colorectal neoplastic polyps: a prospective multicenter study of back-to-back video colonoscopies. *Endoscopy*. 2008;40:284-290.

3. Stoffel EM, Turgeon DK, Stockwell DH, et al. Missed adenomas during colonoscopic surveillance in individuals with lynch syndrome (hereditary nonpolyposis colorectal cancer). *Cancer Prev Res*. 2008;1:470-475.

4. Mecklin JP, Aarnio M, Läärä E, et al. Development of colorectal tumors in colonoscopic surveillance in lynch syndrome. *Gastroenterology*. 2007;133:1093-1098.

5. Rijcken FEM, Hollema H, Kleibeuker JH. Proximal adenomas in hereditary non-polyposis colorectal cancer are prone to rapid malignant transformation. *Gut*. 2002;50:382-386.

6. Corley DA, Jensen CD, Marks AR, et al. Adenoma detection rate and risk of colorectal cancer and death. *N Engl J Med*. 2014;370:1298-1306.

7. East JE, Suzuki N, Stavrinidis M, Guenther T, Thomas HJW, Saunders BP. Narrow band imaging for colonoscopic surveillance in hereditary non-polyposis colorectal cancer. *Gut*. 2008;57:65-70.

8. Ramsoekh D, Haringsma J, Poley JW, et al. A back-to-back comparison of white light video endoscopy with autofluorescence endoscopy for adenoma detection in high-risk subjects. *Gut*. 2010;59:785-793.

9. Chung SJ, Kim D, Song JH, et al. Comparison of detection and miss rates of narrow band imaging, flexible spectral imaging chromoendoscopy and white light at screening colonoscopy: a randomised controlled back-to-back study. *Gut*. 2013;63:785-991.

10. de Vries EGE, Munnink THO, van Vugt MATM, Nagengast WB. Toward molecular imaging–driven drug development in oncology. *Cancer Discovery*. 2011;1:25-28.

11. Hoetker MS, Goetz M. Molecular imaging in endoscopy. *United European Gastroenterol J*. 2013;1:84-92.

12. Staton CA, Chetwood ASA, Cameron IC, Cross SS, Brown NJ, Reed MWR. The angiogenic switch occurs at the adenoma stage of the adenoma carcinoma sequence in colorectal cancer. *Gut*. 2007;56:1426-1432.

13. Hanrahan V, Currie MJ, Gunningham SP, et al. The angiogenic switch for vascular endothelial growth factor (VEGF)-A, VEGF-B, VEGF-C, and VEGF-D in the adenoma-

carcinoma sequence during colorectal cancer progression. *J Pathol*. 2003;200:183-194.

14. van Scheltinga AGTT, van Dam GM, Nagengast WB, et al. Intraoperative near-infrared fluorescence tumor imaging with vascular endothelial growth factor and human epidermal growth factor receptor 2 targeting antibodies. *J Nucl Med*. 2011;52:1778-1785.

15. Cohen R, Stammes MA, de Roos IH. Inert coupling of IRDye800CW to monoclonal antibodies for clinical optical imaging of tumor targets. *EJNMMI* 2011;1:31.

16. Marshall MV, Draney D, Sevick-Muraca EM, Olive DM. Single-dose intravenous toxicity study of IRDye 800CW in Sprague-Dawley rats. *Mol Imaging Biol*. 2010;12:583-594.

17. Zinn KR, Korb M, Samuel S, et al. IND-directed safety and biodistribution study of intravenously injected cetuximab-IRDye800 in cynomolgus macaques. *Mol Imaging Biol*. 2015;17:49-57.

18. van Dam GM, Themelis G, Crane LMA, et al. Intraoperative tumor-specific fluorescence imaging in ovarian cancer by folate receptor-α targeting: first in-human results. *Nat Med*. 2011;17:1315-1319.

19. Themelis G, Yoo JS, Soh K-S, Schulz R, Ntziachristos V. Real-time intraoperative fluorescence imaging system using light-absorption correction. *J Biomed Opt*. 2009;14:064012.

20. Garcia-Allende PB, Glatz J, Koch M, et al. Towards clinically translatable NIR fluorescence molecular guidance for colonoscopy. *Biomed Opt Express*. 2013;5:78-92.

21. Nagengast WB, de Vries EG, Hospers GA, et al. In vivo VEGF imaging with radiolabeled bevacizumab in a human ovarian tumor xenograft. *J Nucl Med*. 2007;48:1313-1319.

22. Eiblmaier M, Meyer LA, Watson MA, Fracasso PM, Pike LJ, Anderson CJ. Correlating EGFR expression with receptor-binding properties and internalization of 64Cu-DOTA-cetuximab in 5 cervical cancer cell lines. *J Nucl Med*. 2008;49:1472-1479.

23. Ferrara N. Vascular endothelial growth factor: basic science and clinical progress. *Endocr Rev*. 2004;25:581-611.

24. Bansal A, Liu X, McGregor DH, Singh V, Hall S. Correlation of epidermal growth factor receptor with morphological features of colorectal advanced adenomas: a pilot correlative case series. *Am J Med Sci*. 2010;340:296-300.

25. Neumann H, Kiesslich R, Wallace MB, Neurath MF. Confocal laser endomicroscopy: technical advances and clinical applications. *Gastroenterology*. 2010;139:388–392.

26. Goetz M, Ziebart A, Foersch S, et al. In vivo molecular imaging of colorectal cancer with confocal endomicroscopy by targeting epidermal growth factor receptor. *Gastroenterology*. 2010;138:435-446.

27. Sturm MB, Joshi BP, Lu S, et al. Targeted imaging of esophageal neoplasia with a fluorescently labeled peptide: first-in-human results. *Sci Transl Med*. 2013;5:184ra61.

28. Joshi BP, Miller SJ, Lee CM, Seibel EJ, Wang TD. Multispectral endoscopic imaging of colorectal dysplasia in vivo. *Gastroenterology*. 2012;143:1435-1437.

29. Miller SJ, Joshi BP, Feng Y, Gaustad A, Fearon ER, Wang TD. In vivo fluorescence-based endoscopic detection of colon dysplasia in the mouse using a novel peptide probe. *PLoS One*. 2011;6:e17384.

30. Bird-Lieberman EL, Neves AA, Lao-Sirieix P, et al. Molecular imaging using fluorescent lectins permits rapid endoscopic identification of dysplasia in Barrett's esophagus. *Nat Med*. 2012;18:315-321.

31. Burggraaf J, Kamerling IMC, Gordon PB, et al. Detection of colorectal polyps in humans using an intravenously administered fluorescent peptide targeted against c-Met. *Nat Med*. 2015;21:955-961.

32. Oosting SF, Brouwers AH, van Es SC, et al. 89Zr-bevacizumab PET visualizes heterogeneous tracer accumulation in tumor lesions of renal cell carcinoma patients and differential effects of antiangiogenic treatment. *J Nucl Med*. 2015;56:63-69.

FIGURE LEGENDS

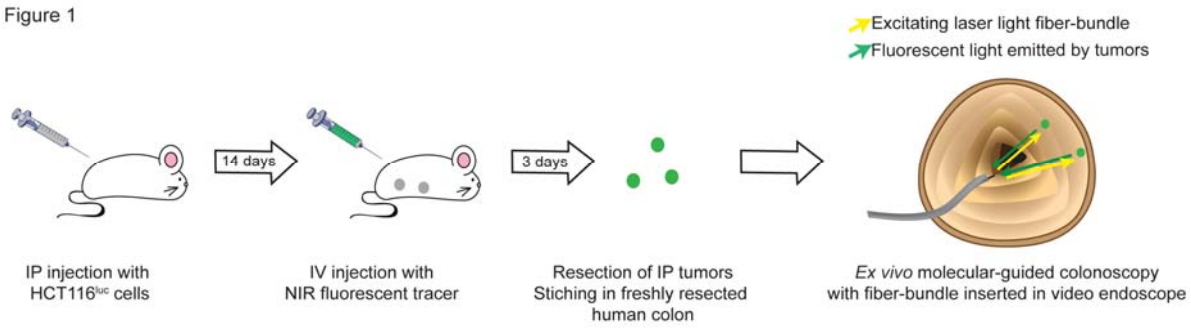

FIGURE 1.

HCT116^{luc} tumor cells were inoculated intraperitoneally (IP) in athymic nude mice. After tumor establishment, the targeted NIR fluorescent tracer (bevacizumab-800CW or cetuximab-800CW), non-targeted NIR fluorescent tracer (IgG-800CW) or sodium chloride was administered intravenously (IV). Three days after administration, IP tumor lesions (diameter of 2-5 mm) were harvested and stitched in a freshly resected human colon. The *ex vivo* molecular-guided colonoscopy procedure was performed using a standard video endoscope with the fiber-bundle of the NIR fluorescence endoscopy platform passed through the working channel.

Figure 2

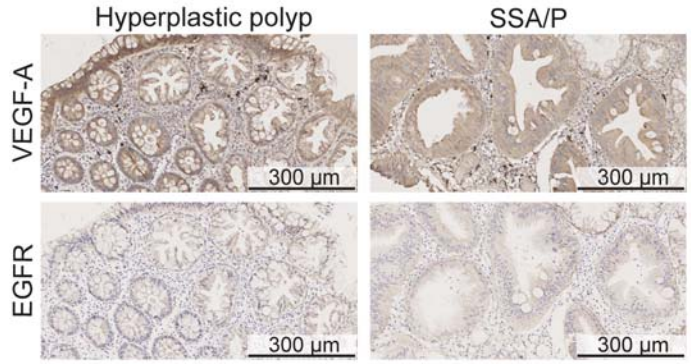

FIGURE 2.

(A) Representative IHC stainings of VEGF-A and EGFR in one hyperplastic polyp and one sessile serrated adenoma/polyp (SSA/P). Both lesions were scored 3 (strong) for VEGF-A and 2 (moderate) for EGFR.

Figure 3

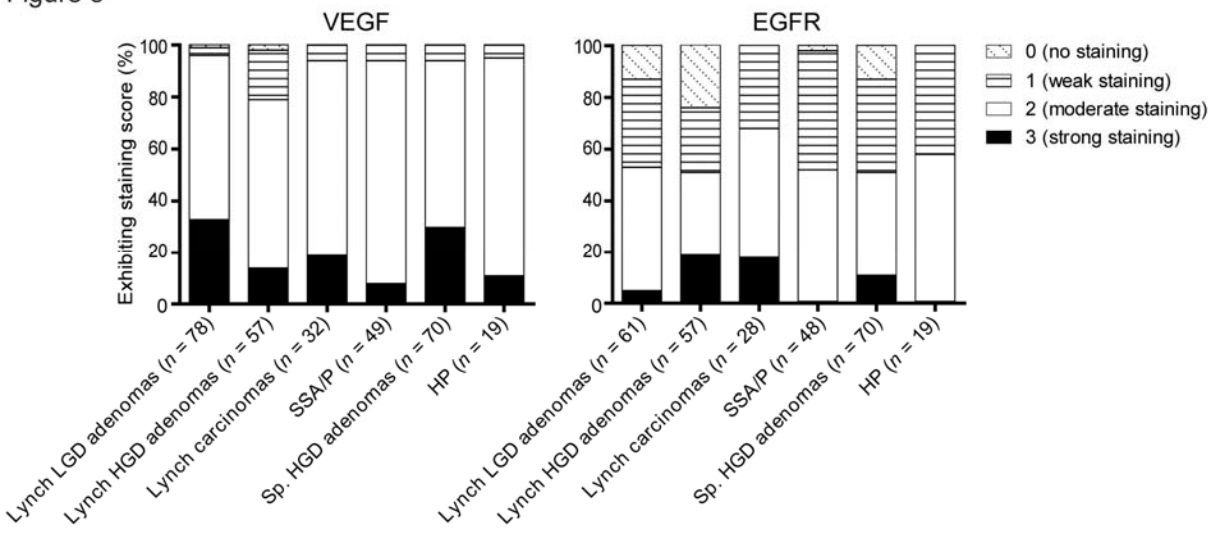

FIGURE 3.

VEGF-A and EGFR expression for colorectal adenomas with low-grade dysplasia (LGD) of patients with Lynch syndrome (LS), adenomas with high-grade dysplasia (HGD) of patients with LS, carcinomas of patients with LS, sessile serrated adenomas/polyps (SSA/P), sporadic adenomas with HGD and hyperplastic polyps (HP).

Figure 4

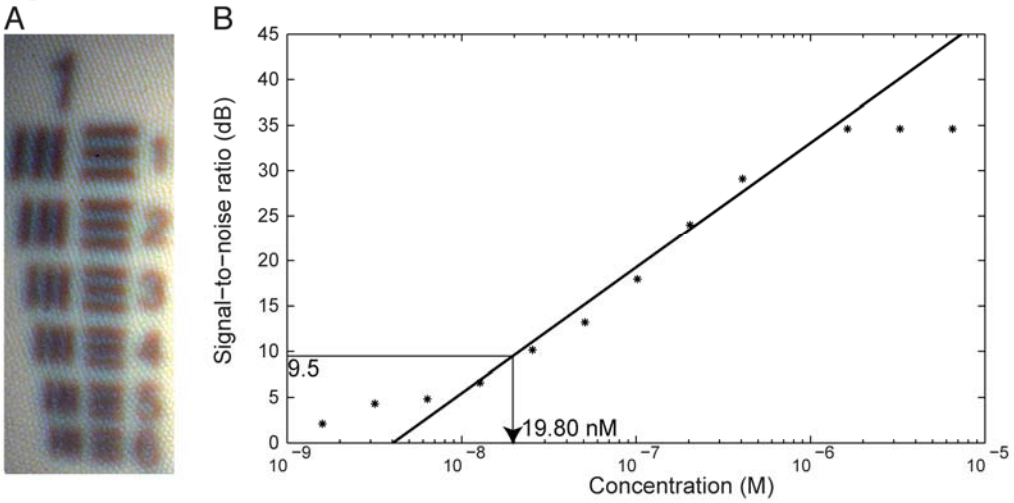

FIGURE 4.

(A) Detail of the USAF 1951 resolution target image, where the vertical and horizontal lines in Element 3 of Group 1 can be distinctly identified, which translates to a spatial resolution of 198.42 μm at a distance of 2 cm. (B) Signal-to-noise ratio over IRDye800CW concentration measured from the dilution series. The detection limit of 9.5 dB lies at a concentration of 19.80 nM.

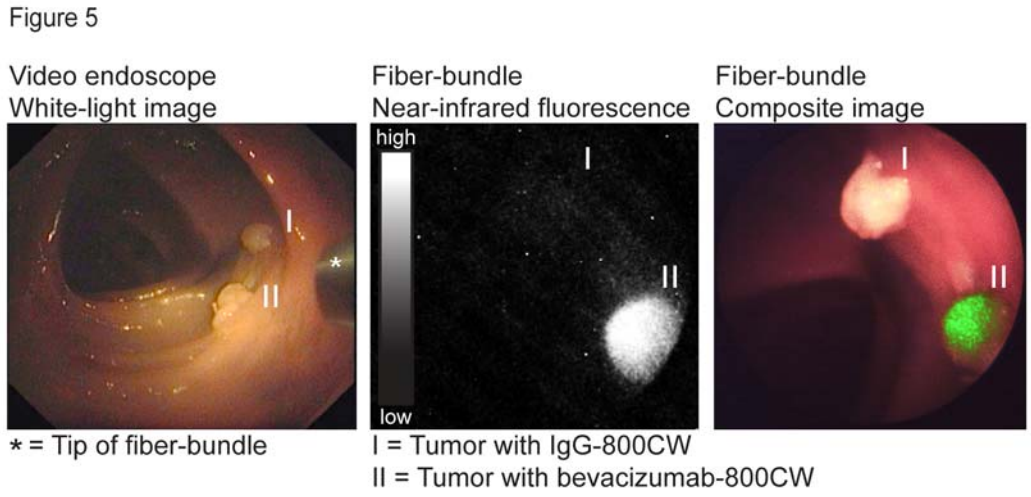

FIGURE 5.

Images acquired during the *ex vivo* molecular-guided colonoscopy of IgG-800CW (I) and bevacizumab-800CW (II) targeted tumors (3x3 mm in size). Endoscopy images were obtained with a video endoscope and the fiber-bundle. The white-light, fluorescence and composite images of the fiber-bundle were real-time projected.

Figure 6

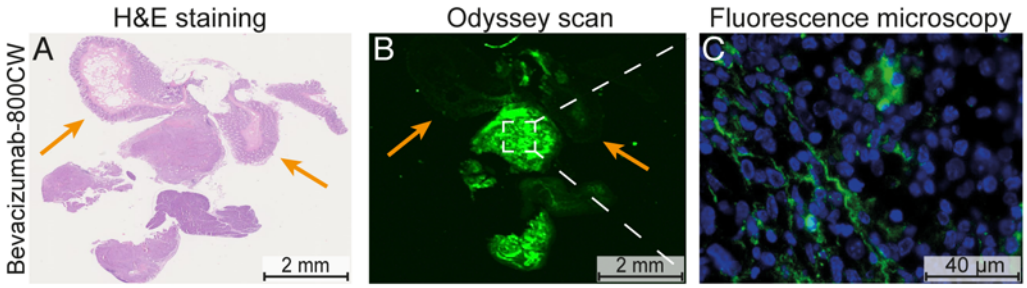

FIGURE 6.

Hematoxylin&eosin (H&E) staining (A), corresponding fluorescence image obtained with Odyssey Scanner (B) and corresponding fluorescence microscopy image (C) of an HCT116^{luc} tumor targeted with bevacizumab-800CW. The Odyssey scan shows clear fluorescence in all tumor tissue at 800nm, while uptake was negligible in the histologic normal tissue (colon and muscle of the mice, see orange arrows). Fluorescence microscopy demonstrated bevacizumab-800CW to be mainly localized in the stroma of the tumors.